

Reduced VLDL clearance in *ApoE*^{-/-}*Npc1*^{-/-} mice is associated with increased *Pcsk9* and *Idol* expression and decreased hepatic LDL-receptor levels

Minako Ishibashi,^{1,*} David Masson,[†] Marit Westerterp,* Nan Wang,* Scott Sayers,* Rong Li,* Carrie L. Welch,* and Alan R. Tall*

Division of Molecular Medicine,* Department of Medicine, Columbia University, New York, NY; and INSERM,[†] Centre de Recherche-UMR866, Faculté de Médecine, Institut Fédératif de Recherche Santé-STIC, Université de Bourgogne, Dijon, France

Abstract Niemann-Pick type C1 (NPC1) promotes the transport of LDL receptor (LDL-R)-derived cholesterol from late endosomes/lysosomes to other cellular compartments. NPC1-deficient cells showed impaired regulation of liver X receptor (LXR) and sterol regulatory element-binding protein (SREBP) target genes. We observed that *ApoE*^{-/-}*Npc1*^{-/-} mice displayed a marked increase in total plasma cholesterol mainly due to increased VLDL, reflecting decreased clearance. Although nuclear SREBP-2 and *Ldlr* mRNA levels were increased in *ApoE*^{-/-}*Npc1*^{-/-} liver, LDL-R protein levels were decreased in association with marked induction of proprotein convertase subtilisin/kexin type 9 (*Pcsk9*) and inducible degrader of the LDL-R (*Idol*), both known to promote proteolytic degradation of LDL-R. While *Pcsk9* is known to be an SREBP-2 target, marked upregulation of IDOL in *ApoE*^{-/-}*Npc1*^{-/-} liver was unexpected. However, several other LXR target genes also increased in *ApoE*^{-/-}*Npc1*^{-/-} liver, suggesting increased synthesis of endogenous LXR ligands secondary to activation of sterol biosynthesis. **In conclusion, we demonstrate that NPC1 deficiency has a major impact on VLDL metabolism in *ApoE*^{-/-} mice through modulation of hepatic LDL-R protein levels. In contrast to modest induction of hepatic IDOL with synthetic LXR ligands, a striking upregulation of IDOL in *ApoE*^{-/-}*Npc1*^{-/-} mice could indicate a role of endogenous LXR ligands in regulation of hepatic IDOL.**—Ishibashi, M., D. Masson, M. Westerterp, N. Wang, S. Sayers, R. Li, C. L. Welch, and A. R. Tall. **Reduced VLDL clearance in *ApoE*^{-/-}*Npc1*^{-/-} mice is associated with increased *Pcsk9* and *Idol* expression and decreased hepatic LDL-receptor levels.** *J. Lipid Res.* 2010. 51: 2655–2663.

Supplementary key words liver • Niemann-Pick disease • receptor • lipoprotein • atherosclerosis • nuclear receptor

This work was supported by National Institutes of Health Grant HL-22682 (A.R.T.) and by the postdoctoral fellowship 09POST2110109 from the American Heart Association (M.W.). Its contents are solely the responsibility of the authors and do not necessarily represent the official views of the National Institutes of Health or other granting agencies.

Manuscript received 13 February 2010 and in revised form 18 June 2010.

Published, JLR Papers in Press, June 18, 2010
DOI 10.1194/jlr.M006163

Copyright © 2010 by the American Society for Biochemistry and Molecular Biology, Inc.

This article is available online at <http://www.jlr.org>

Niemann-Pick type C (NPC) disease is an inherited autosomal recessive cholesterol-storage disorder that involves mutations in *Npc1* or *Npc2* and results in progressive neurological impairment, hepatosplenomegaly, and hepatic dysfunction (1). NPC1 and NPC2 proteins bind LDL-derived free cholesterol in late endosomes/lysosomes (2) and promote its transport to other organelles, including mitochondria, trans-Golgi, endoplasmic reticulum (ER), and plasma membrane. Since NPC1-deficient cells (fibroblasts and macrophages) fail to deliver LDL-derived free cholesterol to mitochondria and ER (3), they have impaired synthesis of endogenous liver X receptor (LXR) ligands, such as 25-hydroxycholesterol (25-OHC) and 27-hydroxycholesterol (27-OHC), and LXR target genes are downregulated (4–6). In contrast, sterol response element binding protein (SREBP)-dependent pathways remain activated because the cleavage of SREBP protein is not suppressed by cholesterol loading (4, 5). While NPC1 deficiency has a major impact on intracellular cholesterol metabolism, its consequences on plasma cholesterol distribution are less clear. Recent work reported that NPC patients show reduced plasma HDL-C and LDL-C levels and increased plasma triglycerides (7–10). In contrast, *Npc1*^{-/-} mice fed a chow diet exhibited increased plasma total cholesterol, mainly in HDL (11–13). Increases in VLDL and LDL cholesterol were observed in *Npc1*^{-/-} mice after high-cholesterol feeding and in the LDL receptor (*Ldlr*)^{+/-}

Abbreviations: 25-OHC, 25-hydroxycholesterol; 27-OHC, 27-hydroxycholesterol; apo, apolipoprotein; CE, cholesteryl ester; ER, endoplasmic reticulum; FCR, fractional catabolic rate; FPLC, fast performance liquid chromatography; HL, hepatic lipase; IDOL, inducible degrader of LDL-R; LDL-R, LDL receptor; LRP1, LDL receptor-related protein 1; LPL, lipoprotein lipase; LXR, liver X receptor; NPC1, Niemann-Pick type C1; PCSK9, proprotein convertase subtilisin/kexin type 9; SR-BI, scavenger receptor class B, type I; SREBP, sterol regulatory element-binding protein; TG, triglyceride.

[†]To whom correspondence should be addressed.
e-mail: ishishiminako@gmail.com

heterozygous genetic background (12, 13). We previously reported that *Apolipoprotein e* (*ApoE*), *Npc1* deficient (*ApoE*^{-/-}*Npc1*^{-/-}) mice fed a chow diet for 12 weeks exhibited accelerated atherosclerosis in proximal aortas as well as an elevation of plasma total cholesterol (14). We recently found that these mice had increased VLDL levels in a Balb/c genetic background. The current study was undertaken to investigate the mechanism underlying the increase of VLDL and IDL/LDL cholesterol concentrations in *ApoE*^{-/-}*Npc1*^{-/-} mice.

MATERIALS AND METHODS

Mice

ApoE^{tm1Unc}/J, *Npc1*^{tm1N/+}/J (*ApoE*^{-/-}*Npc1*^{+/-}) and *Npc1*^{tm1N/+}/J (*Npc1*^{+/-}) mice on the BALB/cNctr background were housed at the Columbia University Medical Center according to the current National Institutes of Health guidelines. All procedures were approved by the Institutional Animal Care and Use Committee. *ApoE*^{-/-}*Npc1*^{+/-} and *Npc1*^{+/-} mice were intercrossed, respectively, to generate *ApoE*^{-/-} and *ApoE*^{-/-}*Npc1*^{-/-} mice, and *Wt* and *Npc1*^{-/-} mice.

Plasma and hepatic lipid measurement

Chow-fed 7-week-old mice were fasted for 5 h and euthanized. Blood and liver were collected. Plasma was separated by centrifugation and stored at -80°C until analyzed. Total plasma cholesterol, phospholipid, HDL cholesterol, and liver cholesterol were measured with Wako enzymatic kits. Plasma and liver triglycerides (TG) were measured with Infinity kits (Thermo Scientific).

Plasma lipid profile analysis by FPLC and ultracentrifugation

100 µl of pooled plasma from 5 h fasted mice (n = 10) was used for fast performance liquid chromatography (FPLC) analysis using a Superose 6 column (GE Healthcare). Cholesterol and TG levels of FPLC fractions were measured using the commercial kits described above. VLDL (d < 1.006 g/ml) was isolated by sequential density ultracentrifugation of plasma using a TLA 100 rotor (Beckmann Coulter Inc.). VLDL was separated using SDS-PAGE and visualized by 0.05% Coomassie Brilliant Blue staining (Sigma-Aldrich).

VLDL-cholesteryl ether turnover study

[³H]cholesteryl ether (CE)-VLDL was generated as previously described (15, 16). Briefly, VLDL (d < 1.006 g/ml) was isolated from 1 ml plasma from *ApoE*^{-/-} or *ApoE*^{-/-}*Npc1*^{-/-} mice by ultracentrifugation. One hundred µCi of cholesteryl hexadecyl ether (cholesteryl-[^{1,2,3}H (N)]palmityl ether) (40–60 Ci/mmol; Perkin Elmer) was added to the lipoprotein solution. *ApoE*^{-/-} and *ApoE*^{-/-}*Npc1*^{-/-} mice (n = 4) were injected with [³H]CE-VLDL (8 × 10⁵ dpm) via the tail vein. After injection, blood was taken from the tail vein at different time points for determination of radioactivity. The fractional catabolic rates (FCR) were calculated from the decay curves of [³H]CE radioactivity in plasma by fitting the data to a biexponential equation according to the method of Matthews. The production rates were calculated by multiplying the FCR by the plasma cholesterol pool and dividing by the body weight.

Isolation of mouse peritoneal macrophages

Peritoneal macrophages were harvested from *ApoE*^{-/-} and *ApoE*^{-/-}*Npc1*^{-/-} mice three days after intraperitoneal injection of thioglycollate. Macrophages were incubated in full medium containing DMEM (25 mM glucose), 10% FBS, and 1% penicillin/streptomycin/glutamine. One h later, nonadherent cells were removed, and adherent cells consisting of macrophages were used for the experiment as described in the figure legends.

Real-time RT-PCR analysis

Liver and peritoneal macrophages were homogenized and total RNA was isolated using the RNeasy mini kit (Qiagen). Total RNA was treated with Turbo DNase (Ambion) and reverse transcribed with Superscript III (Invitrogen). Real-time RT-PCR was performed with SYBR green PCR core reagents (Applied Biosystems). mRNA expression levels were normalized to the 36B4 housekeeping gene.

Western blotting analysis

Total proteins and nuclear extracts (AY2002 nuclear extraction kit; Panomics) from mouse liver were separated (30 µg of protein/sample) by SDS-PAGE and transferred onto nitrocellulose membranes (Bio-Rad). Blots were probed separately with specific antibodies. Following incubation with horseradish peroxidase-conjugated secondary antibodies, proteins were visualized with Amersham ECL advanced western blotting detection kit (GE Healthcare) on X-ray film. Primary antibodies were the following: LDL receptor-related protein (LRP1) (LifeSpan Biosciences); LDL-R, IDOL, SREBP-1, and Lamin A (Abcam);

TABLE 1. Basic characteristics of *ApoE*^{-/-} and *ApoE*^{-/-}*Npc1*^{-/-} mice fed chow diet at 7 weeks of age

Characteristic	<i>ApoE</i> ^{-/-}		<i>ApoE</i> ^{-/-} <i>Npc1</i> ^{-/-}	
	Male	Female	Male	Female
Body weight (g)	24.8 ± 1.2	21.2 ± 1.1	17.9 ± 0.6	16.3 ± 0.8
Liver weight (g)	1.42 ± 0.1	1.19 ± 0.1	1.11 ± 0.1	1.02 ± 0.1
Liver weight / body weight	5.72 ± 0.1	5.58 ± 0.3	6.47 ± 0.4 ^a	6.25 ± 0.1 ^a
Liver				
Cholesterol (mg/g liver)		4.87 ± 0.58		10.15 ± 1.32 ^b
Triglyceride (mg/g liver)		44.21 ± 4.1		7.45 ± 2.6 ^b
Plasma				
Total cholesterol (mg/dl)	548.1 ± 45.2	570.2 ± 40.0	1198.7 ± 68.3 ^b	1234.0 ± 39.3 ^b
Triglyceride (mg/dl)	260.5 ± 38.0	140.3 ± 25.5	158.1 ± 23.2 ^a	98.3 ± 16.4 ^a
HDL-cholesterol (mg/dl)	58.0 ± 7.0	59.4 ± 9.7	149.8 ± 17.6 ^b	160.2 ± 13.7 ^b
Phospholipid (mg/dl)	644.1 ± 32.1		632.7 ± 29.8	
Glucose (mg/dl)	228.5 ± 26.5		180.0 ± 18.5	

apo, apolipoprotein.

^a P < 0.05 versus *ApoE*^{-/-}.

^b P < 0.01 versus *ApoE*^{-/-}.

scavenger receptor class B, type I (SR-BI) (Novus); hepatic lipase (HL) (Santa Cruz); β -actin (Sigma-Aldrich); SREBP-2 (Pharmin-gen); and PCSK9 (kind gift from Dr. Jan L. Breslow at The Rockefeller University). IDOL-positive control is cell lysate from HEK293T cells transfected IDOL/Myip overexpressing plasmid (Novus). IDOL-negative control is cell lysate from HEK293T cells transfected control plasmid.

Lipoprotein lipase activity

Lipoprotein lipase (LPL) activity in plasma was measured with a commercial kit according to the manufacturer's instructions (Roar).

Statistical analysis

Data are shown as mean \pm SEM. Statistical analysis of differences was determined by ANOVA using Bonferroni correction

for multiple comparisons. $P < 0.05$ was considered the threshold for significance.

RESULTS

Total plasma cholesterol levels are significantly higher in $Apoe^{-/-}Npc1^{-/-}$ mice compared with $Apoe^{-/-}$ controls due to an increase in the VLDL fraction

Plasma total cholesterol concentrations were 2-fold higher in $Apoe^{-/-}Npc1^{-/-}$ mice compared with $Apoe^{-/-}$ mice (Table 1). The increase in total cholesterol was more prominent in $Apoe^{-/-}Npc1^{-/-}$ mice in the BALB/cNctr congenic background (current study) than in the 75% C57BL/6, 25% BALB mixed background (see Ref. 14).

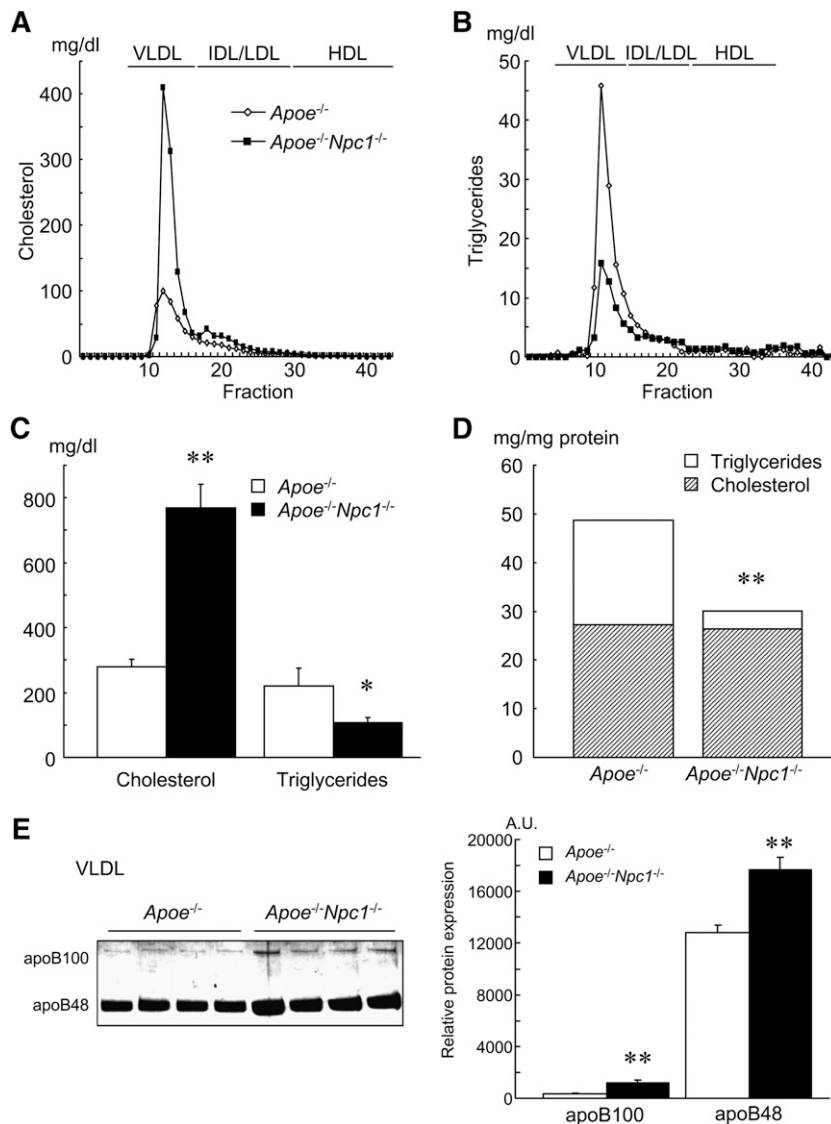


Fig. 1. Plasma lipoprotein profiles in $Apoe^{-/-}$ and $Apoe^{-/-}Npc1^{-/-}$ mice. A and B: Pooled plasma (100 μ l) was used for FPLC analysis (n = 10/group). Distribution of cholesterol (A) and TG (B) among distinct lipoprotein particles. C: Concentration of cholesterol and TG in VLDL separated by ultracentrifugation. D: Concentration of cholesterol and TG corrected for protein in VLDL separated by ultracentrifugation (n = 4/group). * $P < 0.05$, ** $P < 0.01$ versus $Apoe^{-/-}$. E: VLDL isolated by ultracentrifugation was resolved by SDS-PAGE and visualized by Coomassie Blue staining. Each lane represents an individual mouse (n = 4/group). apo, apolipoprotein; FPLC, fast performance liquid chromatography; NPC1, Niemann-Pick type C1; TG, triglyceride.

FPLC analysis showed substantial increases of cholesterol in all lipoprotein fractions in *ApoE*^{-/-}*Npc1*^{-/-} mice, but the most prominent increase was observed in fractions 10–17 corresponding to VLDL (Fig. 1A, C). In contrast, plasma TG concentration and TG in VLDL fractions were reduced in *ApoE*^{-/-}*Npc1*^{-/-} mice (Table 1 and Fig. 1B, C). The cholesterol content of VLDL corrected for protein was similar in both groups of mice, but the concentration of TG was significantly decreased in *ApoE*^{-/-}*Npc1*^{-/-} mice (Fig. 1D). In VLDL separated from plasma by ultracentrifugation, both apoB100 and apoB48 levels were markedly increased in *ApoE*^{-/-}*Npc1*^{-/-} mice, and apoB48 was predominant in both strains (Fig. 1E). The ratio of apoB100/apoB48 was 3.6 in *ApoE*^{-/-}*Npc1*^{-/-} mice compared with 1.4 in *ApoE*^{-/-} mice, showing a predominant increase in apoB100. These results suggest that VLDL and chylomicron remnants depleted in TG are increased in *ApoE*^{-/-}*Npc1*^{-/-} mice.

Cholesterol production is increased and clearance of VLDL-CE is decreased in *ApoE*^{-/-}*Npc1*^{-/-} mice compared with *ApoE*^{-/-} controls

To identify the mechanism responsible for the increased plasma VLDL cholesterol concentration in *ApoE*^{-/-}*Npc1*^{-/-} mice, we analyzed the VLDL-CE clearance and production. We analyzed VLDL-CE clearance by injecting VLDL labeled with [³H]cholesteryl ether into *ApoE*^{-/-} and *ApoE*^{-/-}*Npc1*^{-/-} mice. As shown in Fig. 2, the decay in plasma radioactivity was significantly slower in *ApoE*^{-/-}*Npc1*^{-/-} mice compared with *ApoE*^{-/-} mice, suggesting decreased clearance of VLDL-CE. *ApoE*^{-/-}*Npc1*^{-/-} mice showed a significantly decreased VLDL-CE catabolism with an FCR of 3.61 ± 0.08 pools/d versus 5.73 ± 0.63 pools/d in *ApoE*^{-/-} mice group (*P* < 0.05). Based on pool size and FCR, the calculated CE production rate in *ApoE*^{-/-}*Npc1*^{-/-} mice (152 ± 3.3 mmol/g body weight/day) was significantly increased compared with *ApoE*^{-/-} mice (110 ± 12 mmol/g body weight/day) (*P* < 0.05). Subsequent studies focused on potential mechanisms accounting for the reduction in VLDL-CE clearance.

Hepatic LPL, HL, and apoC expression levels are not different between *ApoE*^{-/-} and *ApoE*^{-/-}*Npc1*^{-/-} mice

LPL and HL can hydrolyze TG in chylomicrons and VLDL, and they act as structural cofactors facilitating cellular uptake of whole lipoprotein particles and selective CE uptake (15, 17). LPL mRNA expression was dramatically increased, but plasma LPL activity was only slightly increased in *ApoE*^{-/-}*Npc1*^{-/-} mice compared with *ApoE*^{-/-} mice (Fig. 3A, B). HL mRNA expression and protein levels in liver were not different between the groups (Fig. 3A, C). These results suggested that LPL and HL were not involved in the accumulation of VLDL-CE in the plasma of *ApoE*^{-/-}*Npc1*^{-/-} mice. Similarly, hepatic mRNA levels of ApoCs and ApoA2, known modulators of plasma VLDL metabolism, were unchanged in *ApoE*^{-/-}*Npc1*^{-/-} mice compared with *ApoE*^{-/-} mice (Fig. 3A).

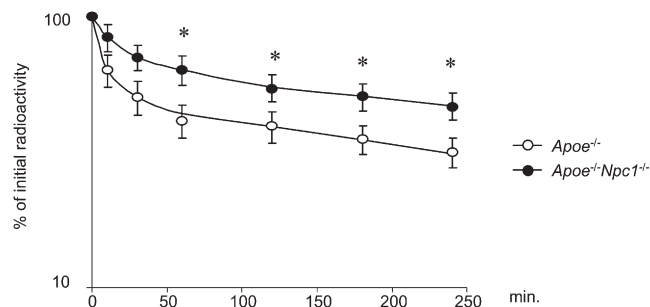


Fig. 2. VLDL-CE clearance. VLDL was isolated from plasma of *ApoE*^{-/-} and *ApoE*^{-/-}*Npc1*^{-/-} mice and radiolabeled. [³H]CE-VLDL was injected in *ApoE*^{-/-} and *ApoE*^{-/-}*Npc1*^{-/-} mice, and the clearance of [³H]CE-VLDL was measured. Values are the fraction of the injected dose remaining at each time point. The curves were fitted using a biexponential equation. Similar results were obtained from two independent experiments. n = 4/group. **P* < 0.05, ***P* < 0.01 versus *ApoE*^{-/-} for the same time point. apo, apolipoprotein; NPC1, Niemann-Pick type C1.

LDL-R protein is decreased in *ApoE*^{-/-}*Npc1*^{-/-} liver despite increased mRNA levels

In the liver, remnant lipoproteins are taken up mainly via the LDL-R pathway, and to a lesser extent, via LRP1, heparin sulfate proteoglycans, and SR-BI (18, 19). LDL-R and LRP1 mRNA expression were significantly increased in *ApoE*^{-/-}*Npc1*^{-/-} liver, whereas SR-BI mRNA levels were unchanged (Fig. 3D). SR-BI protein levels were increased significantly in *ApoE*^{-/-}*Npc1*^{-/-} liver while LRP1 levels were similar between the two groups (Fig. 3E). Strikingly, despite the increased mRNA levels, LDL-R protein levels were significantly decreased in *ApoE*^{-/-}*Npc1*^{-/-} livers, suggesting that LDL-R expression is regulated posttranscriptionally. Therefore, we determined expression levels of PCSK9 and IDOL, which have recently been identified as modulators of LDL-R protein degradation (20, 21). PCSK9 and IDOL mRNA levels as well as protein levels were significantly increased in *ApoE*^{-/-}*Npc1*^{-/-} liver (Fig. 3F, G). These results suggested that increased PCSK9 and IDOL levels diminished LDL-R protein levels and were responsible for the impaired VLDL-CE clearance in *ApoE*^{-/-}*Npc1*^{-/-} mice.

In contrast to the findings in *ApoE*^{-/-}*Npc1*^{-/-} mice, *Npc1*^{-/-} mouse fed a chow diet at 7 weeks of age (Fig. 4A, B) showed no change in LXR-α, SREBP-2, LDL-R, or IDOL gene expression in liver, while PCSK9 gene expression was reduced in *Npc1*^{-/-} liver compared with *Wi* liver. LDL-R and PCSK9 protein levels were similar between groups, and IDOL was decreased in *Npc1*^{-/-} liver. The difference in the results between *Npc1*^{-/-} and *ApoE*^{-/-}*Npc1*^{-/-} mice suggests that hypercholesterolemia induced by *ApoE* deficiency in *Npc1*^{-/-} mice has a key role in determining changes in expression of PCSK9, IDOL, and LDL-R.

NPC1 deficiency induces SREBP-2-dependent and LXR-activated genes and attenuates the SREBP-1c pathway

LDL-R and PCSK9 expression are regulated transcriptionally by SREBP-1a and -2 (22–24), while IDOL was recently reported to be an LXR target gene (20). Therefore, we evaluated the activity of SREBP and LXR pathways in *ApoE*^{-/-}*Npc1*^{-/-}

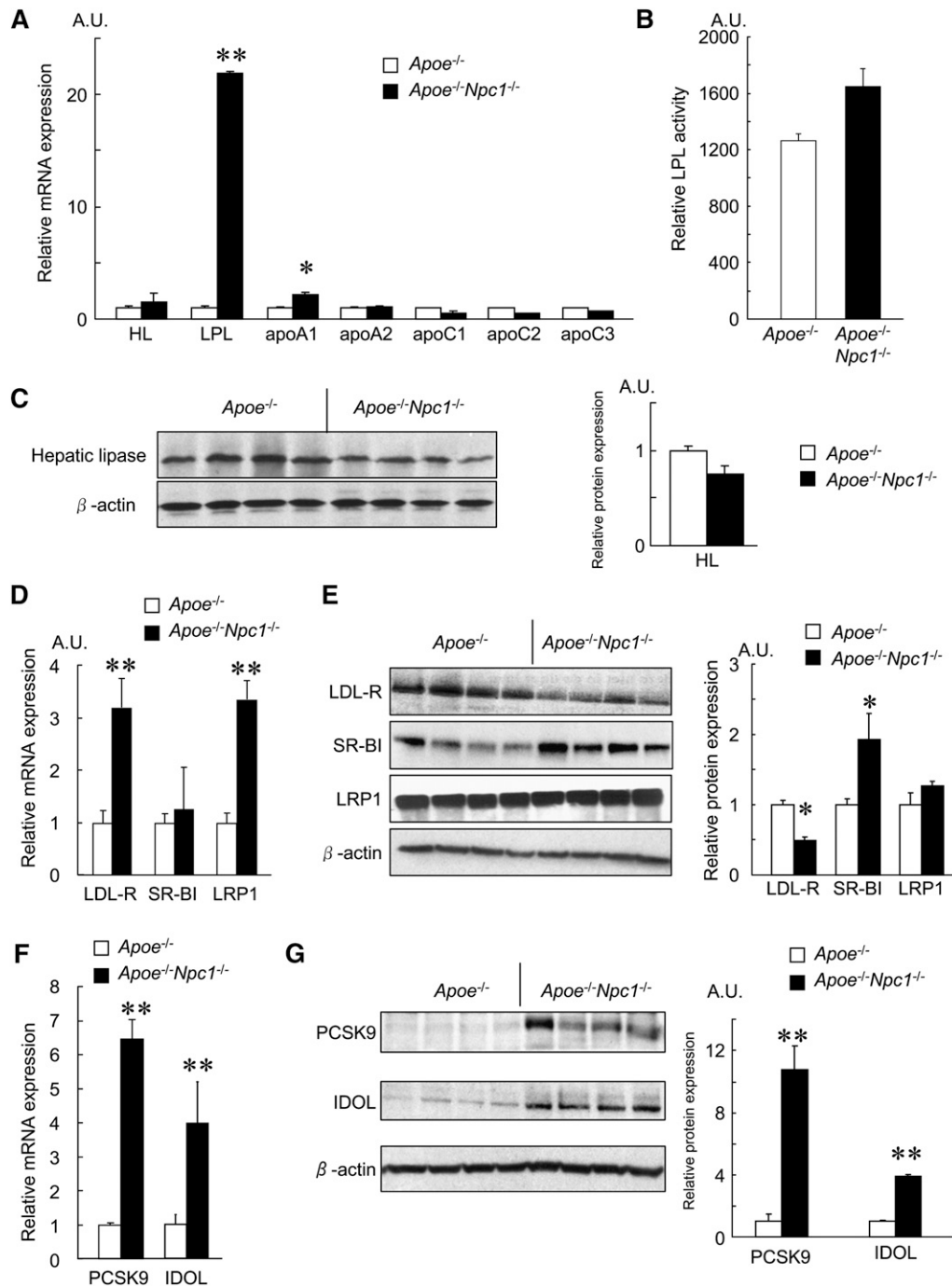


Fig. 3. Hepatic LDL-R protein level is reduced in liver from $Apoe^{-/-}Npc1^{-/-}$ mice compared with $Apoe^{-/-}$ controls. A: Analysis of hepatic mRNA expression of various genes by real-time RT-PCR. B: Plasma LPL activity. C: Western blot analysis of HL and β -actin in liver and quantification by densitometric analysis. D: Analysis of hepatic mRNA expression of various genes by real-time RT-PCR. E: Western blot analysis of LDL-R, SR-BI, LRP1, and β -actin in liver and quantification by densitometric analysis. F: Analysis of hepatic mRNA expression of PCSK9 and IDOL by real-time RT-PCR. G: Western blot analysis of PCSK9, IDOL, and β -actin in liver, and quantification by densitometric analysis. Similar results were obtained from two independent experiments ($n = 4/\text{group}$). * $P < 0.05$, ** $P < 0.01$ versus $Apoe^{-/-}$. apo, apolipoprotein; HL, hepatic lipase; IDOL, inducible degrader of LDL-R; LDL-R, LDL receptor; LPL, lipoprotein lipase; LRP1, LDL receptor-related protein 1; NPC1, Niemann-Pick type C1; PCSK9, proprotein convertase subtilisin/kexin type 9; SR-BI, scavenger receptor class B, type I.

liver. The relative amount of SREBP-1c mRNA was not changed, whereas SREBP-1a mRNA was significantly increased in $Apoe^{-/-}Npc1^{-/-}$ liver compared with $Apoe^{-/-}$ controls (Fig. 5A). As shown in Fig. 5B, nuclear SREBP-1 protein

was significantly decreased in $Apoe^{-/-}Npc1^{-/-}$ liver. Since SREBP-1c is a key lipogenic transcription factor, these results are consistent with the observed decrease of hepatic TG in $Apoe^{-/-}Npc1^{-/-}$ mice (Table 1). On the other hand, SREBP-2

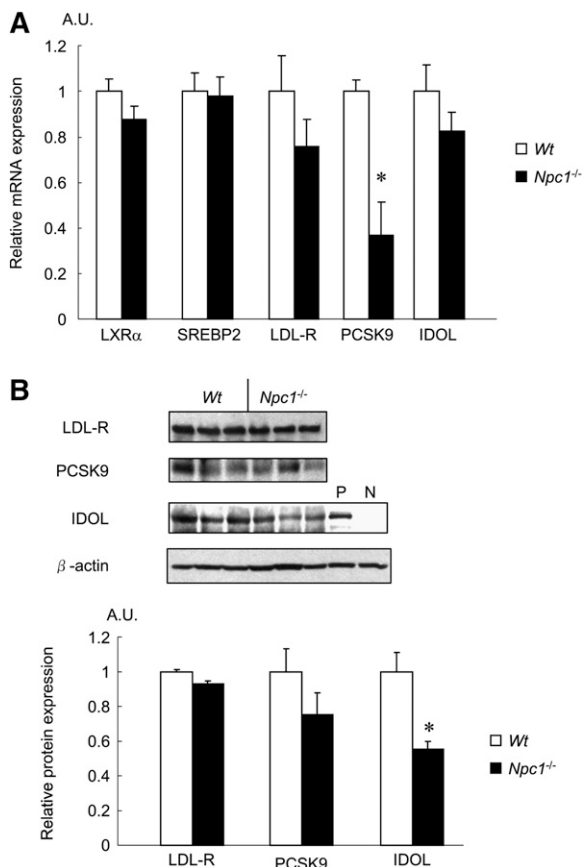


Fig. 4. Hepatic LDL-R, PCSK9, and IDOL protein level in *Wt* and *Npc1*^{-/-} mice. **A:** Analysis of hepatic mRNA expression of LDL-R, PCSK9, and IDOL by real-time RT-PCR. **B:** Western blot analysis of LDL-R, PCSK9, IDOL, and β -actin in liver, and quantification by densitometric analysis. Similar results were obtained from two independent experiments ($n = 3/\text{group}$). "P" means positive control. "N" means negative control. * $P < 0.05$, ** $P < 0.01$ versus *Wt* (wild type). IDOL, inducible degrader of LDL-R; LDL-R, LDL receptor; PCSK9, proprotein convertase subtilisin/kexin type 9; AU, arbitrary unit.

mRNA and nuclear protein levels were dramatically increased in *Apoe*^{-/-}*Npc1*^{-/-} liver (Fig. 5A, B). Accordingly, all SREBP-2 target genes, such as HMG-CoA synthase and HMG-CoA reductase, were also significantly increased in *Apoe*^{-/-}*Npc1*^{-/-} liver (Fig. 5A). These results indicate that SREBP-2 activation is responsible for the increased PCSK9 and LDL-R mRNA levels. LXR α , ABCA1, and ABCG1 were slightly reduced or unchanged in *Apoe*^{-/-}*Npc1*^{-/-} liver compared with *Apoe*^{-/-} controls (Fig. 5C). However, potential LXR-target genes in liver were upregulated in *Apoe*^{-/-}*Npc1*^{-/-} liver, including ABCG8, LPL, and IDOL (Fig. 3A, F and Fig. 5C). In contrast, *Apoe*^{-/-}*Npc1*^{-/-} macrophages showed no significant change of LXR target genes (ABCA1, ABCG1, and IDOL) in the basal state and, as previously observed, failed to induce LXR targets in response to acetylated LDL loading (Fig. 5D).

DISCUSSION

In the current study, we have shown that *Apoe*^{-/-}*Npc1*^{-/-} mice exhibited elevated cholesterol levels but reduced TG levels in both plasma and liver compared with *Apoe*^{-/-} con-

trols. Plasma cholesterol was mainly increased in the VLDL/IDL fractions that were depleted of TG, suggesting remnant accumulation. The accumulation of plasma VLDL cholesterol in *Apoe*^{-/-}*Npc1*^{-/-} mice was partly a result of impaired clearance, likely due to a reduction of hepatic LDL-R protein. While an increase in VLDL-CE production rate was also suggested by the turnover study, this could reflect a decrease in LDL-R protein and increased conversion of slowly cleared, large VLDL into smaller particles (25, 26). mRNA and protein levels of PCSK9 and IDOL, two factors known to promote LDL-R degradation, were elevated. Thus, elevated plasma cholesterol levels in *Apoe*^{-/-}*Npc1*^{-/-} mice are likely due to post-transcriptional downregulation of LDL-R protein.

The increase in nuclear SREBP-2 observed in hepatocytes of *Apoe*^{-/-}*Npc1*^{-/-} is consistent with previous studies in fibroblasts and macrophages (27, 28) and likely accounts for the increase in *Srebf2* expression (Fig. 5A, B) as SREBP-2 targets the promoter of its own gene. While SREBP-2 activation in *Apoe*^{-/-}*Npc1*^{-/-} livers is also likely to explain the increase of PCSK9 levels, the mechanisms that account for IDOL induction are less clear. IDOL/Myliip/MGC11702 has been previously reported to be induced in livers of SREBP-1a transgenic mice (29). Although SREBP-1a mRNA was induced in *Apoe*^{-/-}*Npc1*^{-/-} livers, nuclear SREBP-1 was reduced, and nuclear SREBP-2 was increased. In contrast to findings in SREBP1 transgenic mice, IDOL expression was not increased in liver of SREBP-2 transgenic mice (25), making it unlikely that IDOL was induced by SREBP-2 in our model.

IDOL is known to be a target of LXRs (20). IDOL expression could be increased due to the formation of endogenous LXR ligands in the liver. As a result of increased SREBP-2 gene induction, cholesterol synthesis is likely increased in *Npc1*-deficient hepatocytes, as reflected in the marked increase in HMG-CoA reductase and HMG-CoA synthase mRNAs (Fig. 4A). It has been previously reported that increased endogenous cholesterol synthesis is associated with LXR activation through increased formation of endogenous LXR ligands (30). For example, 24, 25-epoxycholesterol, an intermediate in cholesterol biosynthesis, is a strong LXR activator (31). Levels of cell-associated oxysterols in *Npc1*^{-/-} macrophages were uniformly elevated, even among enzymatically generated side-chain oxysterols 24-OHC, 25-OHC, and 27-OHC (6). We observed that LXR target genes, such as LPL, IDOL, and ABCG8, were induced in the liver of NPC1-deficient mice, suggesting that some LXR target genes are induced. However, expression of other LXR targets, such as ABCA1, ABCG1 and SREBP-1c, was unchanged or even suppressed in *Apoe*^{-/-}*Npc1*^{-/-} liver. Increases in 24, 25-epoxycholesterol have been shown to inhibit the activation of SREBP1c, reflecting induction of Insig-2 (32) and consistent with the changes in the NPC1-deficient livers. In most reports, ABCA1 mRNA is not markedly increased in the liver following LXR activation (33, 34), likely reflecting use of an alternative upstream exon in which the promoter lacks a functional LXRE (35). Hepatic ABCG1 expression is predominantly in Kupffer and endothelial cells rather than

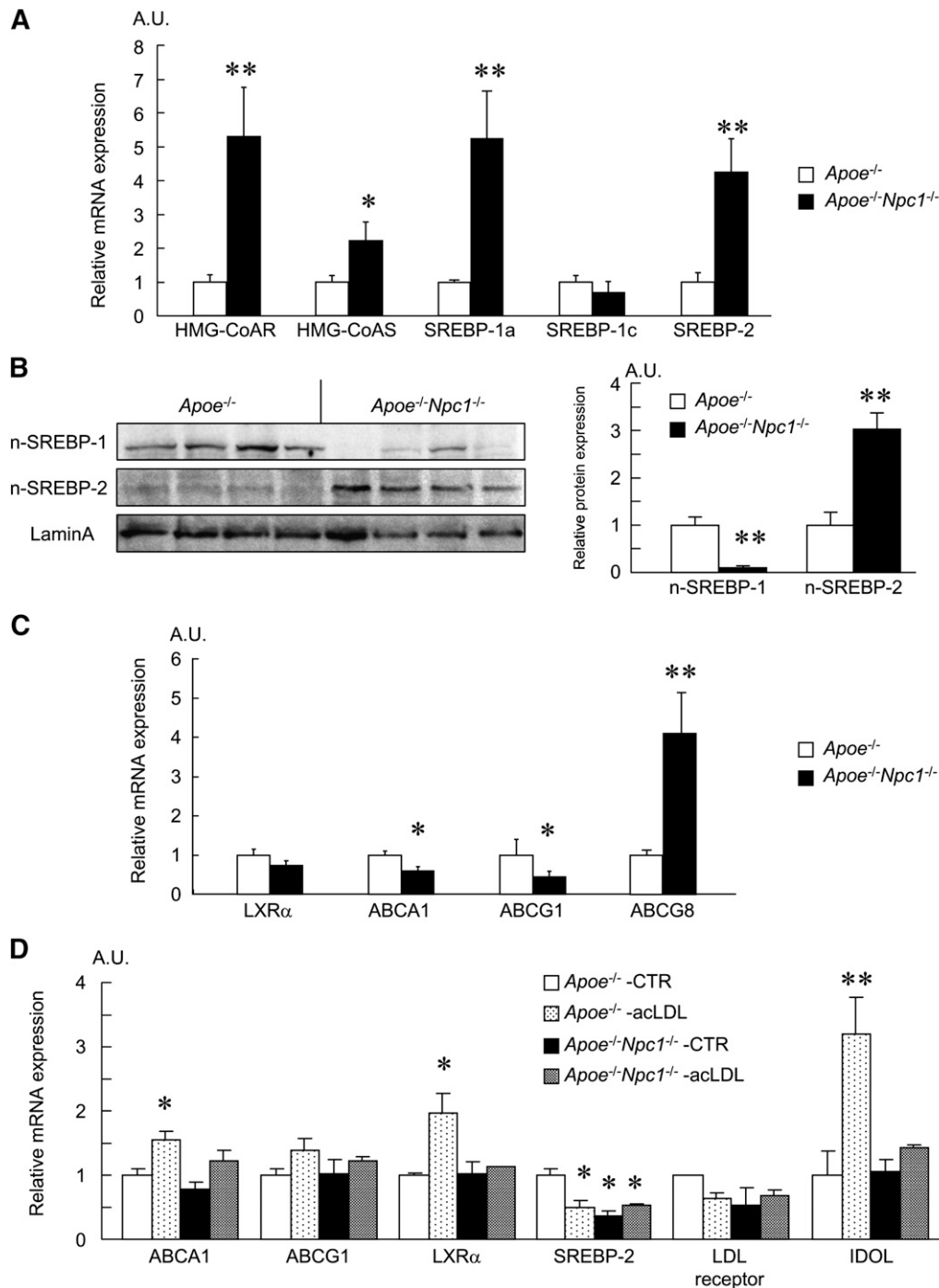


Fig. 5. SREBP-2 processing is increased in liver from *ApoE*^{-/-}*Npc1*^{-/-} mice compared with *ApoE*^{-/-} controls. **A:** Analysis of hepatic mRNA expression of various genes by real-time RT-PCR. **B:** Western blot analysis of nuclear proteins n-SREBP-1 and -2 and Lamin A, and quantification by densitometric analysis. **C:** Analysis of hepatic mRNA expression of various genes by real-time RT-PCR. **D:** Analysis of indicated mRNA expression in peritoneal macrophages by real-time RT-PCR. Peritoneal macrophages were incubated in conditioned medium with or without acetylated LDL (50 μ g/ml) for 24 h. Similar results were obtained from two independent experiments (n = 4/group). **P* < 0.05, ***P* < 0.01 versus *ApoE*^{-/-}. apo, apolipoprotein; LXR, liver X receptor; SREBP, sterol regulatory element-binding protein.


hepatocytes (36). Finally, recent studies have shown that a suppressor microRNA, which targets the mRNA and protein of ABCA1 and ABCG1, is embedded in the *Srebfl2* gene induced in our model (37). These considerations may explain why ABCA1 and ABCG1 mRNAs are not increased,

while other LXR targets, such as ABCG8 and IDOL, are induced in our model.

It is interesting to note that potent synthetic LXR agonists caused only a modest induction of IDOL expression in liver, in contrast to macrophages (20). It is possible that

there are promoter-specific effects of endogenous LXR ligands that account for the induction of IDOL in *Apoe^{-/-}Npc1^{-/-}* mice. While further studies will be needed to clarify the underlying mechanism of IDOL induction in liver, our findings suggest that marked changes in hepatic IDOL expression could represent an important regulatory mechanism that in turn influences cellular levels of LDL-R and circulating levels of atherogenic lipoproteins.

NPC patients show reduced plasma total cholesterol, LDL-C, and HDL-C, and increased TG compared with healthy controls (9, 10). These lipoprotein changes are different from those seen in mice (11–13, 27). This difference could be explained by the many differences between human and mouse lipoprotein metabolism. For example, mice lack the cholesteryl ester transfer protein (CETP), and reduced HDL and LDL cholesterol in humans could in part reflect increased transfer to VLDL mediated by CETP.

In summary, our study provides new insights into the mechanisms linking intracellular cholesterol transport and systemic cholesterol metabolism mediated by IDOL and PCSK9. Our findings add to the clear evidence for SREBP regulation in *Npc1^{-/-}* liver. Although *Npc1^{-/-}* cells fail to produce oxysterol LXR ligands from exogenous cholesterol sources (4–6), our results suggest that alternative endogenous synthetic pathways could activate LXR and induce IDOL expression in liver. It is notable that even though SREBP1c may not be induced by activation of LXRs via 24,25 epoxycholesterol (30), induction of IDOL could lead to increases in plasma LDL, detracting from the usefulness of therapeutic approaches aimed at increases in 24,25 epoxycholesterol (32). 

REFERENCES

- Carstea, E. D., J. A. Morris, K. G. Coleman, S. K. Loftus, D. Zhang, C. Cummings, J. Gu, M. A. Rosenfeld, W. J. Pavan, D. B. Krizman, et al. 1997. Niemann-Pick C1 disease gene: homology to mediators of cholesterol homeostasis. *Science*. **277**: 228–231.
- Kwon, H. J., L. Abi-Mosleh, M. L. Wang, J. Deisenhofer, J. L. Goldstein, M. S. Brown, and R. E. Infante. 2009. Structure of N-terminal domain of NPC1 reveals distinct subdomains for binding and transfer of cholesterol. *Cell*. **137**: 1213–1224.
- Liscum, L., R. M. Ruggiero, and J. R. Faust. 1989. The intracellular transport of low density lipoprotein-derived cholesterol is defective in Niemann-Pick type C fibroblasts. *J. Cell Biol.* **108**: 1625–1636.
- Zhang, J., N. Dudley-Rucker, J. R. Crowley, E. Lopez-Perez, M. Issandou, J. E. Schaffer, and D. S. Ory. 2004. The steroidal analog GW707 activates the SREBP pathway through disruption of intracellular cholesterol trafficking. *J. Lipid Res.* **45**: 223–231.
- Frolov, A., S. E. Zielinski, J. R. Crowley, N. Dudley-Rucker, J. E. Schaffer, and D. S. Ory. 2003. NPC1 and NPC2 regulate cellular cholesterol homeostasis through generation of low density lipoprotein cholesterol-derived oxysterols. *J. Biol. Chem.* **278**: 25517–25525.
- Zhang, J. R., T. Coleman, S. J. Langmade, D. E. Scherrer, L. Lane, M. H. Lanier, C. Feng, M. S. Sands, J. E. Schaffer, C. F. Semenkovich, et al. 2008. Niemann-Pick C1 protects against atherosclerosis in mice via regulation of macrophage intracellular cholesterol trafficking. *J. Clin. Invest.* **118**: 2281–2290.
- Patterson, M. C., A. M. Di Bisceglie, J. J. Higgins, R. B. Abel, R. Schiffmann, C. C. Parker, C. E. Argoff, R. P. Grewal, K. Yu, P. G. Pentchev, et al. 1993. The effect of cholesterol-lowering agents on hepatic and plasma cholesterol in Niemann-Pick disease type C. *Neurology*. **43**: 61–64.
- Shamburek, R. D., P. G. Pentchev, L. A. Zech, J. Blanchette-Mackie, E. D. Carstea, J. M. VandenBroek, P. S. Cooper, E. B. Neufeld, R. D. Phair, H. B. Brewer, Jr., et al. 1997. Intracellular trafficking of the free cholesterol derived from LDL cholesteryl ester is defective in vivo in Niemann-Pick C disease: insights on normal metabolism of HDL and LDL gained from the NP-C mutation. *J. Lipid Res.* **38**: 2422–2435.
- Choi, H. Y., B. Karten, T. Chan, J. E. Vance, W. L. Greer, R. A. Heidenreich, W. S. Garver, and G. A. Francis. 2003. Impaired ABCA1-dependent lipid efflux and hypoalphalipoproteinemia in human Niemann-Pick type C disease. *J. Biol. Chem.* **278**: 32569–32577.
- Garver, W. S., D. Jelinek, F. J. Meaney, J. Flynn, K. M. Pettit, G. Shepherd, R. A. Heidenreich, C. M. Vockley, G. Castro, and G. A. Francis. 2010. The National Niemann-Pick Type C1 Disease Database: correlation of lipid profiles, mutations, and biochemical phenotypes. *J. Lipid Res.* **51**: 406–415.
- Xie, C., S. D. Turley, and J. M. Dietschy. 1999. Cholesterol accumulation in tissues of the Niemann-pick type C mouse is determined by the rate of lipoprotein-cholesterol uptake through the coated-pit pathway in each organ. *Proc. Natl. Acad. Sci. USA*. **96**: 11992–11997.
- Amigo, L., H. Mendoza, J. Castro, V. Quinones, J. F. Miquel, and S. Zanlungo. 2002. Relevance of Niemann-Pick type C1 protein expression in controlling plasma cholesterol and biliary lipid secretion in mice. *Hepatology*. **36**: 819–828.
- Erickson, R. P., A. Bhattacharyya, R. J. Hunter, R. A. Heidenreich, and N. J. Cherrington. 2005. Liver disease with altered bile acid transport in Niemann-Pick C mice on a high-fat, 1% cholesterol diet. *Am. J. Physiol. Gastrointest. Liver Physiol.* **289**: G300–G307.
- Welch, C. L., Y. Sun, B. J. Arey, V. Lemaire, N. Sharma, M. Ishibashi, S. Sayers, R. Li, A. Gorelik, N. Pleskac, et al. 2007. Spontaneous atherothrombosis and medial degradation in *Apoe^{-/-}, Npc1^{-/-}* mice. *Circulation*. **116**: 2444–2452.
- Amar, M. J., K. A. Dugi, C. C. Haudenschild, R. D. Shamburek, B. Foger, M. Chase, A. Bensadoun, R. F. Hoyt, Jr., H. B. Brewer, Jr., and S. Santamarina-Fojo. 1998. Hepatic lipase facilitates the selective uptake of cholesteryl esters from remnant lipoproteins in apoE-deficient mice. *J. Lipid Res.* **39**: 2436–2442.
- Merkel, M., P. H. Weinstock, T. Chajek-Shaul, H. Radner, B. Yin, J. L. Breslow, and I. J. Goldberg. 1998. Lipoprotein lipase expression exclusively in liver. A mouse model for metabolism in the neonatal period and during cachexia. *J. Clin. Invest.* **102**: 893–901.
- Merkel, M., Y. Kako, H. Radner, I. S. Cho, R. Ramasamy, J. D. Brunzell, I. J. Goldberg, and J. L. Breslow. 1998. Catalytically inactive lipoprotein lipase expression in muscle of transgenic mice increases very low density lipoprotein uptake: direct evidence that lipoprotein lipase bridging occurs in vivo. *Proc. Natl. Acad. Sci. USA*. **95**: 13841–13846.
- Fu, T., K. F. Kozarsky, and J. Borensztajn. 2003. Overexpression of SR-BI by adenoviral vector reverses the fibrate-induced hypercholesterolemia of apolipoprotein E-deficient mice. *J. Biol. Chem.* **278**: 52559–52563.
- Van Eck, M., M. Hoekstra, R. Out, I. S. Bos, J. K. Kruijt, R. B. Hildebrand, and T. J. Van Berkel. 2008. Scavenger receptor BI facilitates the metabolism of VLDL lipoproteins in vivo. *J. Lipid Res.* **49**: 136–146.
- Zelcer, N., C. Hong, R. Boyadjian, and P. Tontonoz. 2009. LXR regulates cholesterol uptake through Idol-dependent ubiquitination of the LDL receptor. *Science*. **325**: 100–104.
- Maxwell, K. N., E. A. Fisher, and J. L. Breslow. 2005. Overexpression of PCSK9 accelerates the degradation of the LDLR in a post-endoplasmic reticulum compartment. *Proc. Natl. Acad. Sci. USA*. **102**: 2069–2074.
- Maxwell, K. N., R. E. Soccio, E. M. Duncan, E. Sehayek, and J. L. Breslow. 2003. Novel putative SREBP and LXR target genes identified by microarray analysis in liver of cholesterol-fed mice. *J. Lipid Res.* **44**: 2109–2119.
- Jeong, H. J., H. S. Lee, K. S. Kim, Y. K. Kim, D. Yoon, and S. W. Park. 2008. Sterol-dependent regulation of proprotein convertase subtilisin/kexin type 9 expression by sterol-regulatory element binding protein-2. *J. Lipid Res.* **49**: 399–409.
- Costet, P., B. Cariou, G. Lambert, F. Lalanne, B. Lardeux, A. L. Jarnoux, A. Grefhorst, B. Staels, and M. Krempf. 2006. Hepatic PCSK9 expression is regulated by nutritional status via insulin and sterol regulatory element-binding protein 1c. *J. Biol. Chem.* **281**: 6211–6218.
- Gaw, A., C. J. Packard, G. M. Lindsay, B. A. Griffin, M. J. Caslake, A. R. Lorimer, and J. Shepherd. 1995. Overproduction of small very low density lipoproteins (Sf 20–60) in moderate hypercholesterolemia:

- relationships between apolipoprotein B kinetics and plasma lipoproteins. *J. Lipid Res.* **36**: 158–171.
26. Williams, K. J., R. W. Brocia, and E. A. Fisher. 1990. The unstirred water layer as a site of control of apolipoprotein B secretion. *J. Biol. Chem.* **265**: 16741–16744.
 27. Garver, W. S., D. Jelinek, J. N. Oyarzo, J. Flynn, M. Zuckerman, K. Krishnan, B. H. Chung, and R. A. Heidenreich. 2007. Characterization of liver disease and lipid metabolism in the Niemann-Pick C1 mouse. *J. Cell. Biochem.* **101**: 498–516.
 28. Abi-Mosleh, L., R. E. Infante, A. Radhakrishnan, J. L. Goldstein, and M. S. Brown. 2009. Cyclodextrin overcomes deficient lysosome-to-endoplasmic reticulum transport of cholesterol in Niemann-Pick type C cells. *Proc. Natl. Acad. Sci. USA.* **106**: 19316–19321.
 29. Horton, J. D., N. A. Shah, J. A. Warrington, N. N. Anderson, S. W. Park, M. S. Brown, and J. L. Goldstein. 2003. Combined analysis of oligonucleotide microarray data from transgenic and knockout mice identifies direct SREBP target genes. *Proc. Natl. Acad. Sci. USA.* **100**: 12027–12032.
 30. Yang, C., J. G. McDonald, A. Patel, Y. Zhang, M. Umetani, F. Xu, E. J. Westover, D. F. Covey, D. J. Mangelsdorf, J. C. Cohen, et al. 2006. Sterol intermediates from cholesterol biosynthetic pathway as liver X receptor ligands. *J. Biol. Chem.* **281**: 27816–27826.
 31. DeBose-Boyd, R. A., J. Ou, J. L. Goldstein, and M. S. Brown. 2001. Expression of sterol regulatory element-binding protein 1c (SREBP-1c) mRNA in rat hepatoma cells requires endogenous LXR ligands. *Proc. Natl. Acad. Sci. USA.* **98**: 1477–1482.
 32. Dang, H., Y. Liu, W. Pang, C. Li, N. Wang, J. Y. Shyy, and Y. Zhu. 2009. Suppression of 2,3-oxidosqualene cyclase by high fat diet contributes to liver X receptor-alpha-mediated improvement of hepatic lipid profile. *J. Biol. Chem.* **284**: 6218–6226.
 33. Repa, J. J., S. D. Turley, J. A. Lobaccaro, J. Medina, L. Li, K. Lustig, B. Shan, R. A. Heyman, J. M. Dietschy, and D. J. Mangelsdorf. 2000. Regulation of absorption and ABC1-mediated efflux of cholesterol by RXR heterodimers. *Science.* **289**: 1524–1529.
 34. Tamehiro, N., Y. Shigemoto-Mogami, T. Takeya, K. Okuhira, K. Suzuki, R. Sato, T. Nagao, and T. Nishimaki-Mogami. 2007. Sterol regulatory element-binding protein-2- and liver X receptor-driven dual promoter regulation of hepatic ABC transporter A1 gene expression: mechanism underlying the unique response to cellular cholesterol status. *J. Biol. Chem.* **282**: 21090–21099.
 35. Cavelier, L. B., Y. Qiu, J. K. Bielicki, V. Afzal, J. F. Cheng, and E. M. Rubin. 2001. Regulation and activity of the human ABCA1 gene in transgenic mice. *J. Biol. Chem.* **276**: 18046–18051.
 36. Hoekstra, M., J. K. Kruijt, M. Van Eck, and T. J. Van Berkel. 2003. Specific gene expression of ATP-binding cassette transporters and nuclear hormone receptors in rat liver parenchymal, endothelial, and Kupffer cells. *J. Biol. Chem.* **278**: 25448–25453.
 37. Rayner, K. J., Y. Suárez, A. Dávalos, S. Parathath, M. L. Fitzgerald, N. Tamehiro, E. A. Fisher, K. J. Moore, and C. Fernández-Hernando. 2010. miR-33 contributes to the regulation of cholesterol homeostasis. *Science.* **328**: 1570–1573.